Sub-GHz UWB Biomedical Communication

Mark Stoopman and Wouter A. Serdijn
Biomedical Electronics Group, Electronics Research Laboratory, Delft University of Technology, the Netherlands
mark.stoopman@gmail.nl, w.a.serdijn@tudelft.nl

***Abstract*—This paper proposes the use of sub-GHz impulse radio Ultra-Wideband (UWB) communication for implantable medical devices. This new concept can offer a more reliable, safer and lower power consuming wireless link compared to other biomedical communications today. An operating frequency below 1 GHz is required to minimize the dielectric absorption of the human tissue and simultaneously allows for low power electronics. Investigating the antenna-electronics interface show that a *current* driven antenna results in the most reliable signal transfer. This interface is not bounded to the conventional 50 Ω interface.**

***Index Terms*—Sub-GHz, UWB, biomedical, wireless communication, implantable medical device, antenna, current driven**

I. Introduction

The microelectronic revolution combined with the advances in chemistry, molecular biology and medicine will have a huge impact on the medical world in the near future. Deep brain stimulation, personalized drug delivery, and patient monitoring are just a few applications in this multibillion-dollar market. Medical implantable devices with wireless communication allow doctors to monitor and adjust the treatment of their patients without any further surgical procedure. This wireless link should be safe, reliable and power efficient. Today, wireless biomedical communication is achieved by inductive coupling or narrow band communication.

Inductive coupling has the advantage that no battery is required, thus ensuring a long lifetime. However, the communication range is limited to a few cm's and is sensitive to the position of the external coil. Depending on the quantity to be measured, this can make health monitoring an inconvenient and time consuming process.

Narrow band communication uses a higher carrier frequency and is based on far field wave propagation. This extends the wireless link range and also results in an increase of bandwidth. The drawback is that narrow band communication can suffer from frequency selective fading. Furthermore, unpredictable variations in the electrical properties of the body can cause a shift in the antenna resonance frequency, making it difficult to match. Finally, it is not very power efficient since traditional narrow band communication uses a continuous wave, resulting in continuous power consumption.

To overcome these problems, we propose sub-GHz UWB biomedical communication. UWB impulse radio uses carrierless, short duration pulses with possibly a very low duty cycle (<1%). This allows for an ultra-low power system with a very low average emission level. High bit rates can be achieved because of the large bandwidth. Another advantage is that UWB impulse radio has a high level of multipath immunity. The antenna-electronics interface is also more robust against variation of the tissue, since the information is spread out over a wide frequency range. Moreover, operating below 1 GHz puts less demands on the electronic circuits in terms of operating current. This in combination with the excellent tissue penetration makes it a good candidate for biomedical communication.

In this paper, the characteristics of human tissue are investigated in Section 2. In Section 3, an equivalent antenna circuit model is developed and possible driving signal quantities are discussed. Section 4 shows the implantable antenna simulation results. A link budget analysis is presented in Section 5. Finally, the conclusions are given in Section 6.

II. Human Tissue

The biomedical communication channel under consideration exists of the implanted medical device, the human body and the surrounding area of the patient. Tissue properties may vary with patient dependent on weight, health, age, position and sex, making it difficult to predict the channel. Still, we need to have an estimation of how much power at which frequency is lost to determine the best operating frequency band.

The dielectric properties of the tissues can be modeled using the complex relative permittivity given in [1]

$$\epsilon_r(j\omega) = \epsilon_\infty + \sum_{n=1}^{5} \frac{\epsilon_s - \epsilon_\infty}{1 + j\omega\tau_n} + \frac{\sigma_i}{j\omega\epsilon_0} \tag{1}$$

where ϵ is the permittivity $[\mathrm{F/m}]$, $\sigma(\omega)$ is conductivity $[\mathrm{S/m}]$, τ_n is the time constant $[\mathrm{s}]$ and ω is the angular frequency $[\mathrm{rad/s}]$.

The one-dimensional layered tissue model shown in Figure 1 is used to study the power loss. We assume that the implant is located closely underneath the skin. In this model the plane wave enters perpendicular to an isotropic, homogeneous medium and propagates from inside the muscle tissue, making a transition to fat, skin and finally free space. The other two dimensions extend to infinity.

978-1-4244-7268-0/10/$26.00 ©2010 IEEE

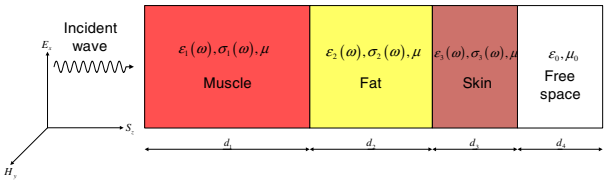

Figure 1: One-dimensional layered tissue model.

Note that this is an extremely simplified model, but it gives a rough estimation of the power loss over a broad frequency range.

In this analysis we define a uniform plane wave which only has an x-component (electric field) and y-component (magnetic field) that are both function of the propagation direction z only.

$$\mathbf{E} = \hat{E}_x e^{-\gamma z}\mathbf{a}_x \tag{2}$$

$$\mathbf{H} = \hat{H}_y e^{-\gamma z}\mathbf{a}_y \tag{3}$$

The propagation coefficient $\gamma\ [\mathrm{m}^{-1}]$ is dependent on the medium and is given by $\gamma = \sqrt{j\omega\mu_0\mu_r\left(\sigma + j\omega\epsilon_0\epsilon_r\right)}$ [2]. The solution of this complex square root can be written as $\gamma = \alpha + j\beta$, where

$$\alpha = \frac{\omega}{c}\sqrt{\frac{\epsilon_r\mu_r}{2}\left[\sqrt{1+\left(\frac{\sigma}{\omega\epsilon_r\epsilon_0}\right)^2}-1\right]} \tag{4}$$

$$\beta = \frac{\omega}{c}\sqrt{\frac{\epsilon_r\mu_r}{2}\left[\sqrt{1+\left(\frac{\sigma}{\omega\epsilon_r\epsilon_0}\right)^2}+1\right]} \tag{5}$$

Calculating the power loss involves determining the transmission coefficient of each medium transition. The transmission coefficient of the wave propagating from Medium 1 to Medium 2 is defined as the ratio of the transmitted to the incidental field. Using the boundary conditions, we can write the electric field transmission coefficient as

$$\hat{T}_E = \frac{\hat{E_x}^t}{\hat{E_x}^i} = \frac{2\eta_2}{\eta_1+\eta_2} \tag{6}$$

where $\eta = \sqrt{\frac{j\omega\mu}{\sigma+j\omega\epsilon}}$ is the wave impedance in $[\Omega]$. Similarly, we can write the magnetic field transmission coefficient

$$\hat{T}_H = \frac{\hat{H_y}^t}{\hat{H_y}^i} = \frac{2\eta_1}{\eta_1+\eta_2} \tag{7}$$

By calculating the time-averaged power density $S\left[\mathrm{W/m^2}\right]$ of the wave in Media 1 and 2, we can determine the power loss. The real time-averaged power density in Medium 2 is

$$S_2 = \frac{1}{2}\mathrm{Re}\left[\hat{\mathbf{E}}_2 \times \hat{\mathbf{H}}_2^*\right] = S_1\mathrm{Re}\left[\hat{T}_E\hat{T}_H^*\right]e^{-2\alpha_2 z} \tag{8}$$

The power transfer factor A_T is found when substituting Equations 6 and 7 in 8:

$$A_T = \frac{S_2}{S_1} = 4\frac{\mathrm{Re}\left[\eta_1\eta_2^*\right]}{|\eta_1+\eta_2|^2}e^{-2\alpha_2 z} \tag{9}$$

For an n-layered tissue model A_T can be written as:

$$A_T = \prod_{i-1}^{n} 4\frac{\mathrm{Re}\left[\eta_{i-1}\eta_i^*\right]}{|\eta_i+\eta_{i-1}|^2}e^{-2\alpha_i d_i} \tag{10}$$

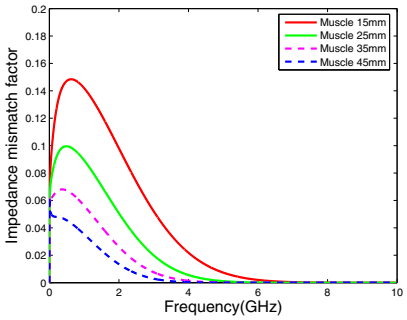

Figure 2: Power transfer factor for a muscle-fat (15mm)-skin (1.5mm)-free space layered tissue model with varying muscle thickness.

To demonstrate the variation in tissue, the muscle thickness is varied from 15 to 45 mm. Looking at the total power transfer in Figure 2 we conclude that there is an optimum power transfer factor around approximately 600 MHz. As expected, the power loss increases at high frequencies. It is also noted that increasing the layer thickness or adding another layer will decrease and shift the frequency response to lower frequencies. However, this analysis does not include the influence of the antenna itself. This will be discussed in the next sections.

III. Implantable Antennas

In this work we visualize the antenna and body as one radiating structure. Hence, the antenna characteristics are influenced by the patient. The antenna determines the antenna-electronics interface, operating frequency band, power level and will also dominate the occupied area of the implanted communication system. Because of its importance, it is required to have a firm understanding of the implantable antenna characteristics. To have an estimation of the maximum allowed antenna dimensions we had a private conversation with neurosurgeon Prof. Dirk de Ridder from the University Hospital Antwerp. From his personal experience, a maximum dimension of two stacked 2 euro coins can be inserted into the skull for neurostimulation in the brain. We will use these dimensions as a reference throughout this paper.

As an experiment we fabricated and measured the input impedance of three types of UWB antennas. We used planar UWB dipole antennas because they have good performance in terms of input impedance, gain, efficiency and size. The antennas where fabricated on a FR4 Printed Circuit Board (PCB) using [3] to determine the dimensions of the antennas. The dimension of the PCB are 26x26x1.6 mm, roughly the size of a 2 euro coin. The PEMA 2 antenna dimensions in Figure 3a are: F=2mm, G=1mm, L=7mm, H=2mm, R=8mm.

The major to minor axial ratio of the elliptical antennas are 1:25 and 1:5. The typical electrical properties of the used PCB are $\epsilon_r = 4.3$ and loss parameter $\tan\delta = 0.01$ at 1 GHz.

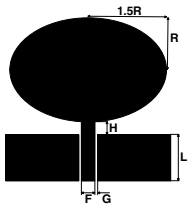

(a) PEMA 2 antenna dimensions.

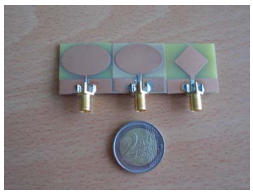

(b) Variety of fabricated antennas.

Figure 3: Planar UWB dipole antennas.

Measurements

We used muscle simulating liquid and raw pork meat to represent the human body. The simulating liquid consists of de-ionized water, sugar, salt and hydroxyethylcellulose (HEC). The percentage of each ingredient for a frequency range of 100MHz to 1GHz can be found in [4].

The impedance measurements of various antennas inserted in pork meat and simulating liquid are shown in Figure 4. Note that the resistance of all antennas are almost constant over a frequency range of 300-900 MHz. The resistance is significantly smaller compared to the reactance, which is to be expected of an electrically small antenna.

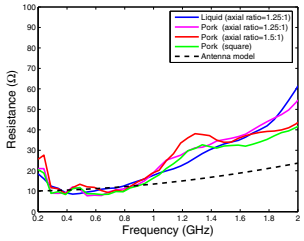

(a) Measured real impedance

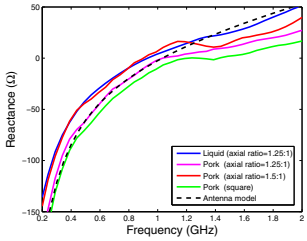

(b) Measured imaginary impedance

Figure 4: Various measured antenna impedances in pork and muscle simulating liquid.

An equivalent RLC circuit has been developed to model the antenna impedance in the frequency range of 300-900 MHz. The dotted black line in Figure 4 is the impedance of the equivalent circuit depicted in Figure 5. The resistance R_A can be seen as the radiation resistance. The radiated power is represented by the power dissipated in this resistance.

Antenna driving signal quantity

The conventional way of driving any antenna is to use an impedance matched network to obtain maximum power transfer and to prevent reflections. The required characteristic impedance is frequently assumed to be 50 Ω without any further discussion. In this design, no transmission lines are needed since the chip will be integrated into the antenna.

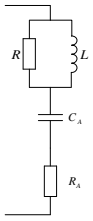

Figure 5: Antenna equivalent circuit model for 300-900 MHz, $R_A = 10\,\Omega$, $C_A = 4$ pF, $R = 400\,\Omega$, $L = 6$ nH.

The physical length of the wire is therefore only a few mm. In other words, working below 1 GHz allows us to assume that the voltage and current along the wire are constant and we do not have to be concerned about propagation effects.

The demand to maximize power transfer also does not apply in this design. Though it may be convenient from a measurement point of view to standardize on characteristic impedances, there seems to be no fundamental reason why an antenna should be terminated for optimum power transfer. Actually, power transfer is a very inefficient way of signal processing since at each interface, half of the available signal power is lost. Also, the signal transfer becomes inaccurate due to the variation in matching network and antenna impedance. The performance of the wireless link should not rely on how well the antenna is impedance matched. Hence, the designer has to *choose* which signal quantity represents and transfers the information in the most accurate way.

The physical information is represented by the power in the radiation resistance R_A, which can be delivered by a voltage, current or impedance matched power source, all three shown in Figure 6. When looking at the model in Figure 5, it suggests to drive it with a *current*. This guarantees that the desired power is always delivered to the radiation resistance, independent of the reactance. This result is very compatible with electronics since transistors are natural current sources.

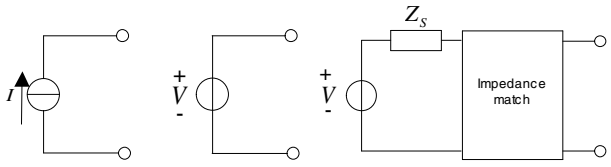

(a) Current (b) Voltage (c) Power

Figure 6: Antenna driving signal quantities.

IV. Simulation Results

Knowing the antenna impedance doesn't tell us anything about the radiation characteristics. Small electrical antennas are often referred to be inefficient radiators because of their low radiation resistance and large reactance, making them difficult to match. In this section we will investigate if this is also true for a current driven antenna. The antenna used in the measurements is simulated inside the same muscle-fat-skin-free space layered tissue model using CST Microwave Studio 5.0.2.

Simulations showed that for frequencies higher than 500 MHz, the antenna itself is a very efficient radiator ($\eta \approx 90\%$) despite its low radiation resistance. The *total* efficiency includes the external impedance mismatch and dielectric absorption. This impedance mismatch can be significant. However, a current driven antenna does not suffer from impedance mismatch. Simulations also showed that the implantable antenna has an typical dipole radiation pattern below 1 GHz but quickly deviates from this with increasing frequency. This is another good argument to use sub-GHz UWB communication.

Figure 7a shows the simulated antenna gain. It is evident that the optimum operating frequency lies higher than the calculated 600 MHz in Section 2. This can be explained since the analytical results in Section 2 were obtained without taking the antenna into account.

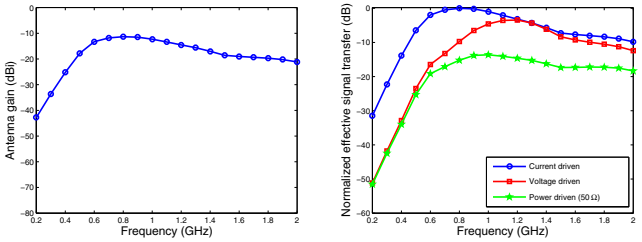

(a) Maximum antenna gain (b) Effective signal transfer

Figure 7: Simulated implanted antenna.

The antenna gain is independent of the driving source because antenna gain is defined as the ratio between the radiated power and the accepted power in a certain direction and does not include the interface losses.

To have a fair comparison between the different driving quantities, the signal reduction along the path between the source and the antenna must be included. The normalized effective signal transfer shown in Figure 7b relates the driving signal quantity to the far field radiated power. Clearly, the current driven antenna is preferred. It must be noted that no impedance matching network has been used for the power driven antenna. However, the maximum signal transfer will never be higher than a current driven antenna, even with an ideally impedance matched antenna.

V. Link Budget

In the link budget shown in Table I we assume On-Off Keying (OOK) with a non-coherent receiver. We aim for a low bit rate in the order of 1 Mb/s. A center frequency of 750 MHz with a -10 dB 500 MHz bandwidth has been chosen as operating band. We used a Gaussian pulse as input signal with a duration of 6 ns and a peak current of 5.5 mA. This is considered acceptable since new types of lithium batteries such as lithium carbon monofluoride (CFx) batteries offer a high energy density and can be pulsed at currents above 20 mA [5]. Note that the average current drawn from the battery is considerably less because the duty cycle is only 0.6%, ensuring ultra-low power consumption. Figure 8a shows the simulated radiated electric field strength at 5 meter.

Table I: Link Budget

Term	*Data*	*Unit*	*Comment*
Transmitter calculations			
$P_{Tx,pulse}$	-12.6	dBm	Tx average pulse power
G_{Tx}	-15	dB	Tx antenna gain
PL_{FS}	43.4	dB	Free space path loss at 5 m
L_{Add}	20	dB	Additional losses (indoor path loss, patient movement)
Receiver calculations			
G_{Rx}	2	dB	Rx antenna gain
P_{Rx}	-89	dBm	Received power
N_0	-174	dBm/Hz	Noise power spectral density
N_b	-114	dBm	Noise power per bit ($N_b = N_0 + 10\log_{10}(R_b)$)
NF	5	dB	Rx noise figure
P_n	-109	dBm	Total average noise power per bit
E_b/N_0	17	dB	Energy per bit per noise PSD
IL	3	dB	Receiver implementation loss
P_{Sens}	-89	dBm	Receiver sensitivity

Although it shows some small distortion, the original Gaussian shape is clearly present. The corresponding PSD shows that some headroom is left with respect to the FCC mask. This allows for higher pulse power or higher bit rates.

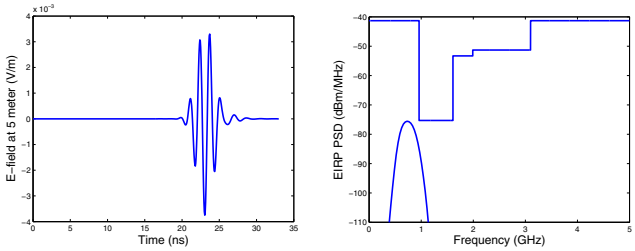

(a) Radiated E-field at 5 meter. (b) PSD and FCC mask

Figure 8: Radiated pulse with corresponding PSD.

VI. Conclusions

The concept of using sub-GHz UWB biomedical communication has been presented. The advantage of operating below 1 GHz has been proved with analytical, measurement and simulation results. An antenna equivalent circuit model has been developed which directly lead to the conclusion that a current driven antenna results in the most reliable signal transfer, eliminating the need for conventional 50 Ω matching. Finally, a realistic link budget analysis showed that sub-GHz UWB communication is a feasible concept.

References

[1] S. Gabriel, R.W. Lau and C. Gabriel, "*The dielectric properties of biological tissues:III.Parametric models for the dielectric spectrum of tissues,*"Phys. Med. Biol.,vol. 41, 1996.

[2] M.D. Verweij, P.M. van den Berg, H. Blok, "*Electromagnetic Waves, An Introductory Course*", Delft University Press, ISBN 90-407-1836-9, 1999

[3] K.P. Ray, "*Design Aspects of Printed Monopole Antennas for Ultra-Wide band Applications*", SAMEER, IIT Campus, Hill Side, Powai, Mumbai 400076, India, 2008

[4] Jack J. Wojcik, Paul G. Cardinal, "*Tissue Recipe and Calibration Requirements SSI/DRB-TP-D01-033*", Spectrum Sciences Institute RF Dosimetry research Board,Canada, 1998

[5] V. S. Mallela, V. Ilankumaran and N.S. Rao, "*Trends in Cardiac Pacemaker Batteries*", Indian Pacing and Electrophysiology Journal (ISBN 0972-6292), 4(4): 201-212, 2004